We are IntechOpen, the world's leading publisher of Open Access books Built by scientists, for scientists

6,900
Open access books available

186,000
International authors and editors

200M
Downloads

154
Countries delivered to

Our authors are among the

TOP 1%
most cited scientists

12.2%
Contributors from top 500 universities

CLARIVATE ANALYTICS
BOOK CITATION INDEX
INDEXED

WEB OF SCIENCE™

Selection of our books indexed in the Book Citation Index
in Web of Science™ Core Collection (BKCI)

Interested in publishing with us?
Contact book.department@intechopen.com

Numbers displayed above are based on latest data collected.
For more information visit www.intechopen.com

Coplanar-Microstrip Transitions for Ultra-Wideband Communications

Mohammed El-Gibari, Dominique Averty, Cyril Lupi,
Yann Mahé Hongwu Li and Serge Toutain
Institut de Recherche en Electrotechnique et Electronique de Nantes Atlantique
University of Nantes, Faculté des Sciences et Techniques
France

1. Introduction

Nowadays optics is penetrating into the broadband access networks, so the data transmission bit-rate can be guaranteed regardless the distance between the subscriber and the central office. Many laboratories are working on the radio over fiber technology in the home networks. For home network applications, one must use low-cost and broadband modulators to transcribe the electrical signal into optical signal. The electro-optic polymers on which very active research is being carried out have the required properties for realizing this kind of modulators. Their realization needs a certain number of delicate manufacturing steps, therefore, a rigorous study of the component must be made before the realization of the modulators. The optimization of the modulator optical structure must be made first, from the properties of polymers at one's disposal and the technological constraints, in order to obtain a single mode guide with minimum losses. Then, optimization of the driving electrode, inseparable step from the optical study, should be carried out. In electro-optic modulators based on polymer, the chromophore molecules responsible for the electro-optic effect are oriented perpendicularly to the substrate as they are generally poled by Corona effect or with contact electrodes. Consequently, a microstrip line is suitable to apply the driving signal to induce the electro-optic effect. Before packaging the final component, it is necessary to assess its performances directly on wafer by use of a probe station, usually equipped with probes compatible with coplanar lines GSG (Ground-Signal-Ground) insuring an easy electrical contact. So, a transition between coplanar and microstrip lines (CPW-MS) is indispensable to characterize the components on wafer. This transition must satisfy at least these three criteria: ultra-wideband, easy to realize and low-cost. One solution is to physically connect the coplanar ground planes to the bottom ground plane of the microstrip line through a via-hole, which would make the component more expensive without eliminating all parasitic resonance (Haydl, 2002). It is in this context that we conducted a comprehensive study of via-free transitions between coplanar and microstrip lines, in order to make easy and simple the characterization of components driven by microstrip line with CPW (Coplanar waveguide) probes. These transitions may be also employed in all microwave circuits driven by microstrip lines.

2. Constraints related to modulator packaging

The electro-optical (EO) polymers are expected to allow realizing cheaper modulators with much better performances than those based on inorganic crystals such as $LiNbO_3$ (Courjal et al., 2002) and semiconductors such as GaAs (Kim et al., 1990). Among the advantages of polymers, we can quote the very broad bandwidth thanks to a good optical-microwave phase matching (Chen et al., 1997), low driving voltage due to high electro-optic coefficient (>100 pm/V) (Dalton et al., 1999), low cost and compatibility of integration with semiconductor materials (Faderl et al., 1995).

The realization of modulators on EO polymer entails the following manufacturing stages. The first stage is to deposit a thin films polymer by spin-coating in order to realize a Mach-Zehnder interferometer structure with two buried rectangular single-mode waveguide arms. In our case, this constraint dictates the choice of the cladding polymers which confines the optical wave in the electro-optical polymer. Once the single-mode optical waveguide is made, the second step consists in realizing the driving electrode which apply the control voltage and thus modulate the light. The overlap between the optical and microwave waves and the impedance matching are two important elements to take into account to determine the dimensions of this electrode. These dimensions affect also the Y junctions of the Mach-Zehnder electro-optical modulator. Figure 1 shows the structure of a modulator based on EO polymer.
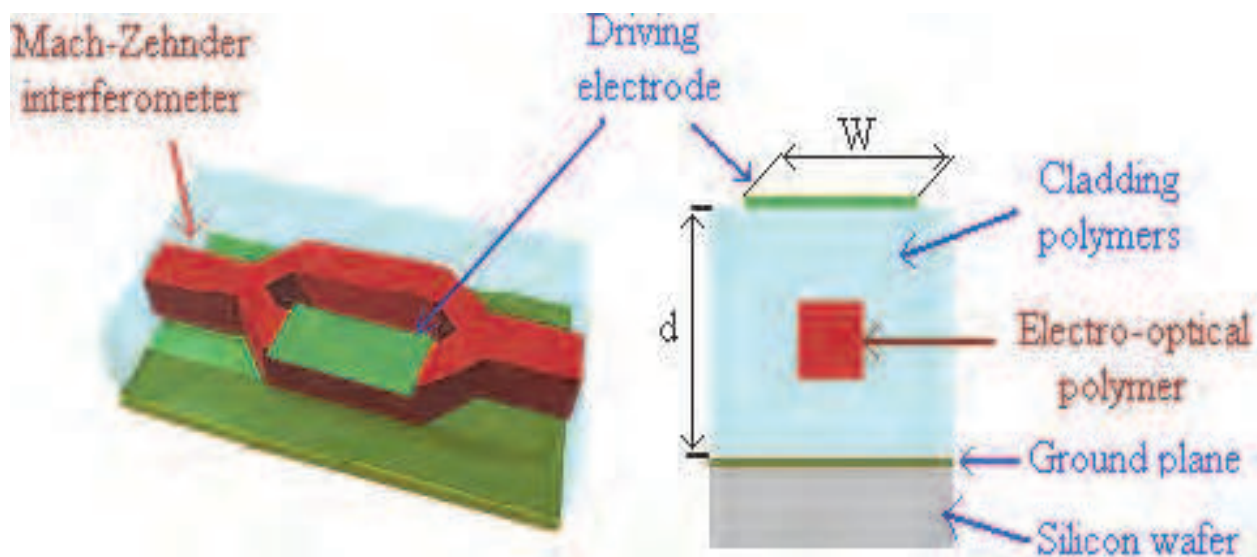

Fig. 1. Overview of the structure of an electro-optical modulator based on polymer

Optimization of modulator design consists in an optimal trade-off between the following main characteristics: high electro-optical bandwidth, low driven voltage, low optical insertion loss and high modulation ratio. The driving voltage V_π is a key parameter in the optical optimization of the component. It is defined as the voltage introducing a phase shift of π between the two arms of the Mach-Zehnder interferometer. This voltage depends on the light wavelength (λ), the refractive index (n), the gap distance (d) between signal and ground electrodes, the interaction length (L) between the optical and electrical waves, the overlap integral between them (Γ) and the electro-optical coefficient (r). This voltage is given when ignoring the microwave signal attenuation:

$$V_\pi = \frac{\lambda d}{n^3 r L \Gamma} \tag{1}$$

The major challenge is to minimize this voltage while keeping the optical insertion loss as low as possible. But these constraints are often contradictory. On one hand, an increase of the interaction length (L) minimizes certainly the driving voltage. But, the electrical losses will increase which limits the bandwidth of the component. On the other hand, the decrease of the gap distance between signal and ground electrodes reduces the optical wave confinement and results in larger absorption of evanescent wave by the electrode. The compromise to be found between a low driving voltage and a high bandwidth is a crucial point when designing electro-optical modulators.

Taking into account the characteristics and properties of polymers employed and in order to optimize the modulator driving voltage, the thickness of polymers (d) is usually fixed between 8 and 10 µm (Michalak, et al., 2006). Once the dimensions of the optical structure are fixed, it is then necessary to optimize the driving electrode in order to maximize the electro-optical effect of the modulator. Indeed, the bandwidth of the component depends on the type and the characteristics of the microwave electrode. In the case of electro-optical modulators based on polymer, the chromophores responsible for the electro-optic effect are oriented perpendicularly to the substrate as they are generally poled by Corona effect or with contact electrodes. So, in order to obtain maximum electro-optic effect, the driving electric field must be oriented as the chromophores. Consequently, a microstrip line is suitable to apply the driving signal. It is therefore necessary to optimize this microstrip line to maximize the overlap factor between optical and electrical waves and maintain its characteristic impedance around 50 Ω to avoid any reflection of the signal. Figure 2 shows the variation of the characteristic impedance of a microstrip line according to the ratio of width (W) / thickness (d) and for different relative permittivities according to the analytical equations of Wheeler and Hammerstad (Wheeler, 1977 & Hammerstad, 1975):

$$Z_c = \frac{Z_0}{2\pi\sqrt{\varepsilon_r}} \ln\left[C\frac{d}{W} + \sqrt{1 + \left(\frac{2d}{W}\right)^2} \right] \tag{2}$$

$$C = 6 + (2\pi - 6)\exp\left(-\left(30.666\frac{d}{W}\right)^{0.7528}\right) \tag{3}$$

Z_0 = characteristic impedance of vacuum

Taking into account the low relative permittivity of polymer between 2.5 and 4 (Algani, et al., 2005), a ratio (W/d) between 2 and 3 is required to have the impedance of microstrip line around 50 Ω, that's to say an electrode width W ranging between 16 µm and 30 µm.

Once the dimensions of the optical guides and microwave driving electrode are optimized, the next step is to make this modulator usable for industrial customers. Thus, for the component packaging, in addition to the dimensions, it is also necessary to take into account the inputs and outputs of the component: one optical input and one optical output via optical fiber pigtails, a microwave connector that gives access to the driving electrode and DC connectors which make possible to bring some functionalities, bias and chirping for example.
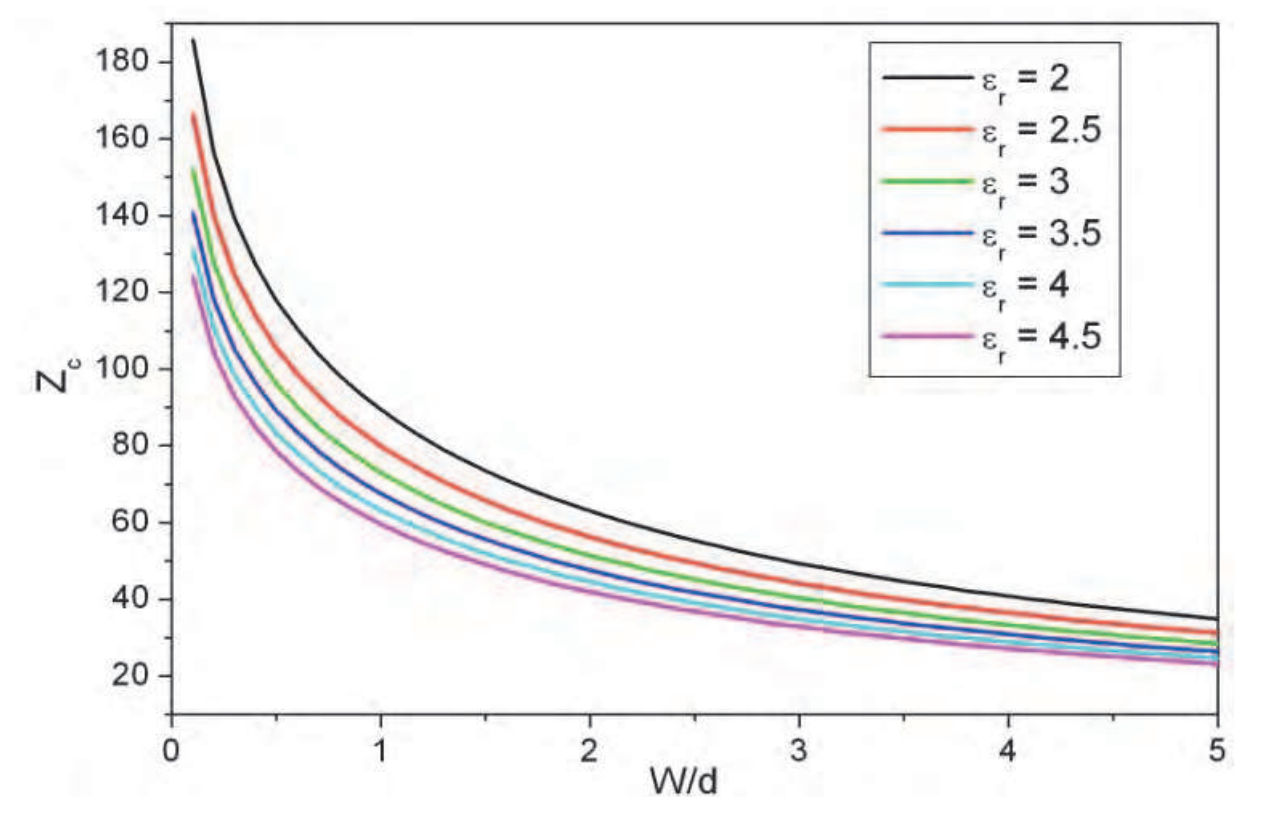
Fig. 2. Variation of characteristic impedance of a microstrip line according to the ratio W/d and for different relative permittivities.
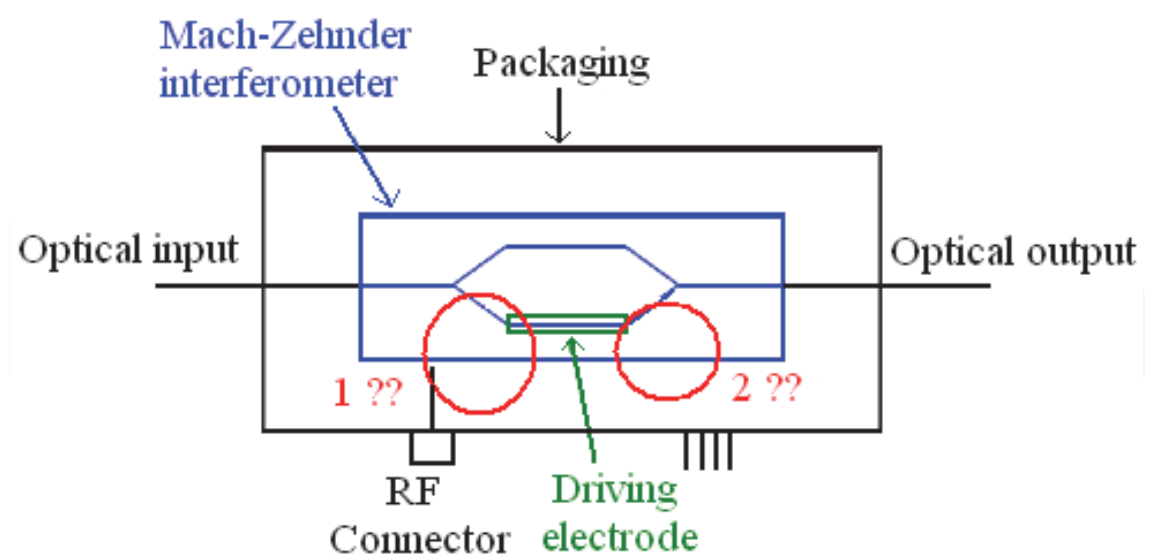

Fig. 3. Packaging of an electro-optical modulator based on polymer

Figure 3 shows a complete diagram of a modulator packaging (in black on the figure) in which we depict the structure of Mach-Zehnder interferometer in blue and the microstrip driving electrode in green. In this type of components, optical accesses will be privileged because of the strong constraints related to their dimensions. In general, the optical coupling

is made by lensed fiber allowing the injection of the light in the optical guide and collecting it at the output of the Mach-Zehnder interferometer. After a dynamic alignment, these last can be fixed at the package by using an epoxy adhesive or by brazing of a metallic coating deposited on the optical fiber by using a laser source. As to the microwave accesses, it will be necessary to connect the driving electrode to a connector whose axis is perpendicular to this microstrip line (cf. red section (1) in figure 3) and to connect the other end of the microstrip line (cf. red section (2) in figure 3) to a 50 Ω load in order to avoid signal reflection. Usually, in planar technology, broadband 50 Ω load is realized with a thin resistive film deposited on an alumina substrate and etched by laser ablation with the necessary dimensions. But that requires the realization of metalized holes, which is very difficult in our case (cf. figure 4).
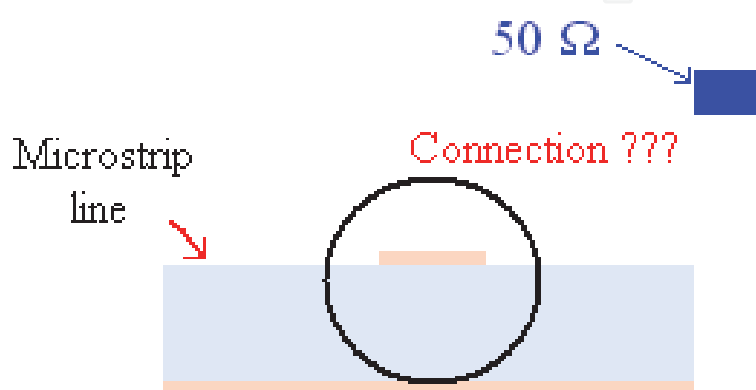

Fig. 4. Difficulty related to the interconnection of a load on a microstrip line

An easy way is to put two 100 Ω loads on a coplanar structure. They are in parallel and thus make it possible to load the microstrip line by a 50 Ω impedance (cf. Figure 5). In this case, the problem then is to realize a connection between the coplanar line and the microstrip line (red section in figure 5).
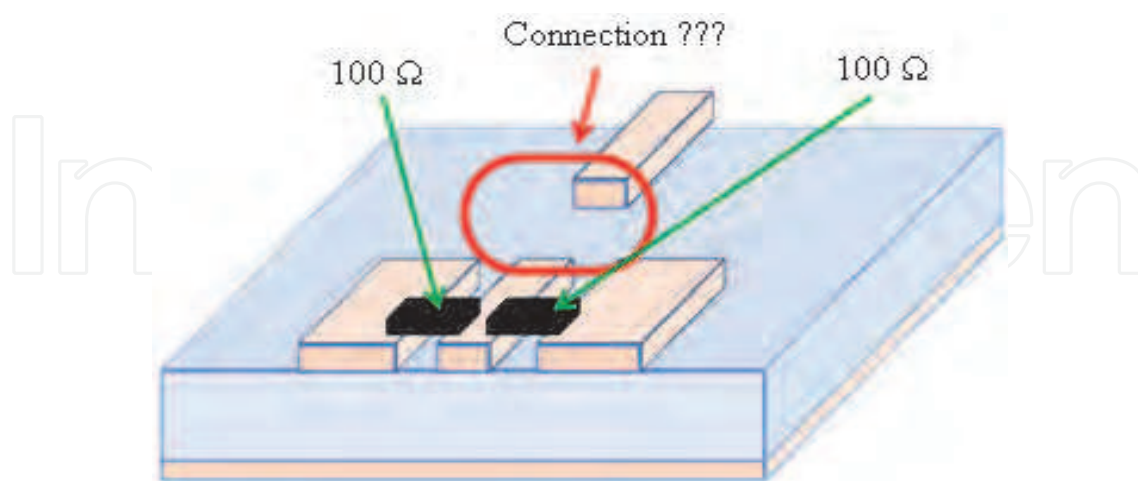

Fig. 5. Connection of a 50 Ω load realized with two 100 Ω loads connected in parallel on a coplanar line.

To launch a microwave signal from a generator to the component driving electrode (cf. red section (1) in figure 3), appropriate connectors are necessary. Indeed, with a coaxial cable,

the interior radius of its outer conductor should be approximately equal to the substrate thickness. In the case of a thin substrate, as shown in figure 6, the most of energy is reflected because of the dimensional difference between the substrate thickness and the connector contact. This mismatch can cause difficulties for electrical contact during microwave packaging and seriously degrade device performance.
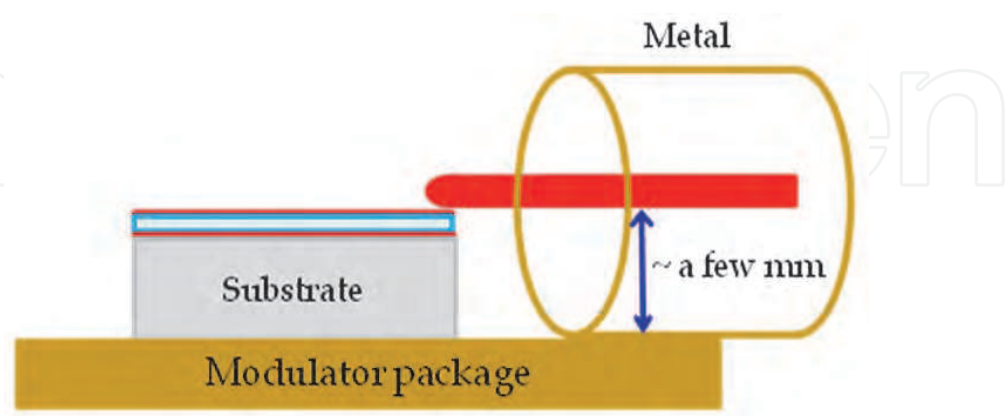

Fig. 6. Constraint related to the excitation of a structure in thin layer by a coaxial connector

Thus, to avoid mismatch problems, it is preferable to use a coplanar connector like the end launch coplanar connector, Model #1492-04A-5 of SouthWest Microwave (Figure 7). In this case, the impedance matching between the connector and the driving electrode is realized by a transition between the quasi-TEM mode of the coplanar line and that of the microstrip line.
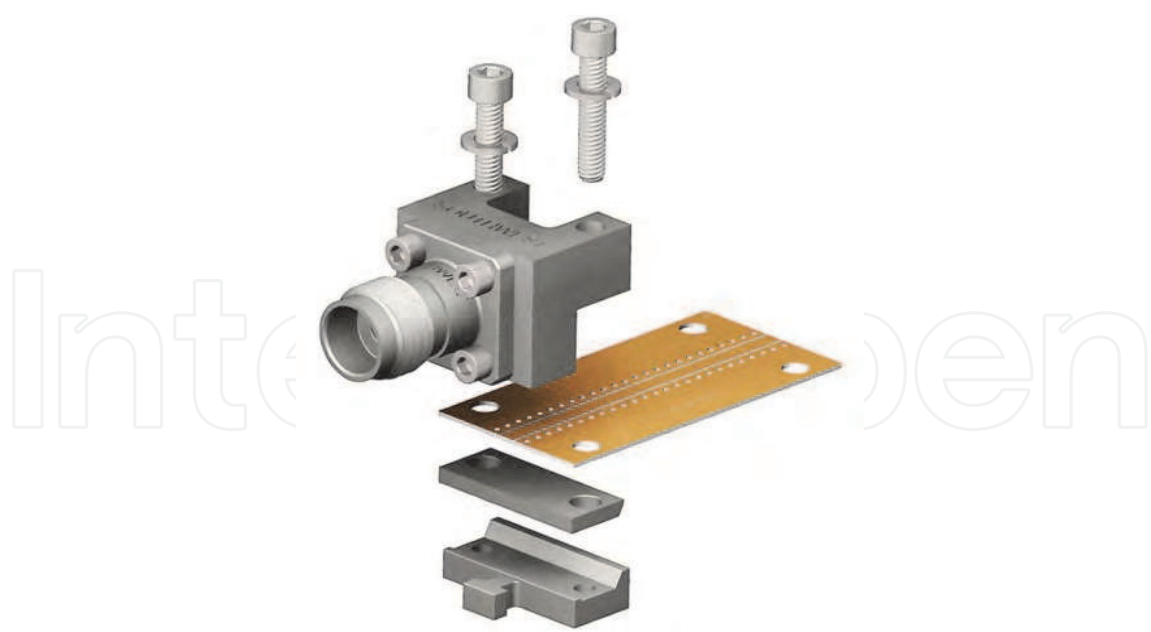

Fig. 7. The end launch coplanar connector, Model #1492-04A-5 of SouthWest Microwave [DC - 50 GHz]

So, due to the low thickness of polymer substrate, a coplanar to microstrip transition is needed for both modulator packaging and on-wafer measurement of the electro-optic

modulator before the packaging steps. As a result, we will attach ourselves to study ultra-broad bandwidth vialess coplanar-microstrip-coplanar (CPW-CPW-MS) transition on thin polymer substrate.

First, we will optimize back-to-back GCPW-MS-GCPW (Grounded Coplanar Waveguide-Microstrip lines) transitions without via-hole in the substrate to connect upper and lower ground plane and without patterning the bottom ground plane. These transitions use the electromagnetic coupling between the bottom and top ground planes. In the second part, we study the transitions for component connectorization using coplanar connectors. At this stage, patterning of the bottom ground plane is necessary to maintain the characteristic impedance to 50 Ω. So, an optimization of the dimensions of these transitions is essential for easy installation of the coplanar connectors and packaging component.

3. Coplanar-microstrip (GCPW-MS) transitions

3.1 GCPW-MS-GCPW transitions on the thick substrate

In the literature, several structures have been proposed to realize vialess CPW-MS transitions according to the intended application and the desired bandwidth (Zheng, et al., 2003 & Safwat, et al., 2002 & Lee, et al., 2006 & Gauthier, et al., 1998). Most of these vialess transitions are realized on standard commercial 635-μm substrates. With this thickness, coplanar-microstrip transitions are generally "easier" to realize, in terms of etching, that those on thin films. We essentially focus our attention on the transitions proposed by Strauss (Straub, et al., 1996) and Zhu (Zhu & Melde, 2006). The structures 1 and 2, shown in figure 8, have the advantage of a homogeneous lower ground plane. Their coplanar section is so grounded coplanar waveguide (GCPW). The first proposed structure with coplanar pads has limited bandwidth when it is realized with thick substrates. The bandwidth extension can be then obtained by using the second transition with radial stubs. The structure 3 proposed by Zhu gives promising bandwidth. However, this transition requires patterning the bottom ground plane which complicates the manufacturing process. To compare the performances of these transitions in the same configuration, we have calculated their performances, by numerical simulation with the help of HFSS, in back to back configuration on the commercial PTFE/glass/ceramic NH9338 substrate with a thickness of 254 μm (ε_r = 3.41 and Tanδ = 0.0047). This substrate is chosen because of its low relative permittivity near to that of polymers. For our simulations, we took a standard thickness of the copper of 18 μm.

In order to maintain the characteristic impedance matching to 50 Ω, the dimensions of each transition were first calculated using Linecalc software of Agilent Advanced Design System. The optimal dimensions of each transition are listed in Table 1.

Structure 1	Structure 2	Structure 3
L = 2 cm, L1 = 2 mm, G = 150 μm, W = 1.4 mm and S = 2 mm	L = 2 cm, R = 1.5 mm, G = 150 μm, W = 1.4 mm, S = 0.5 mm Stub angle = 30°	W1 = 1 mm, W2 = 1.2 mm, W3 = 1.4 mm, G1 = 125 μm, G2 = 140 μm, G3 = 1 mm Lg1 = Lg2 = Lg3 = 0.75 mm, L = 2 mm, S1 = 1.5 mm and S2 = 0.5 mm

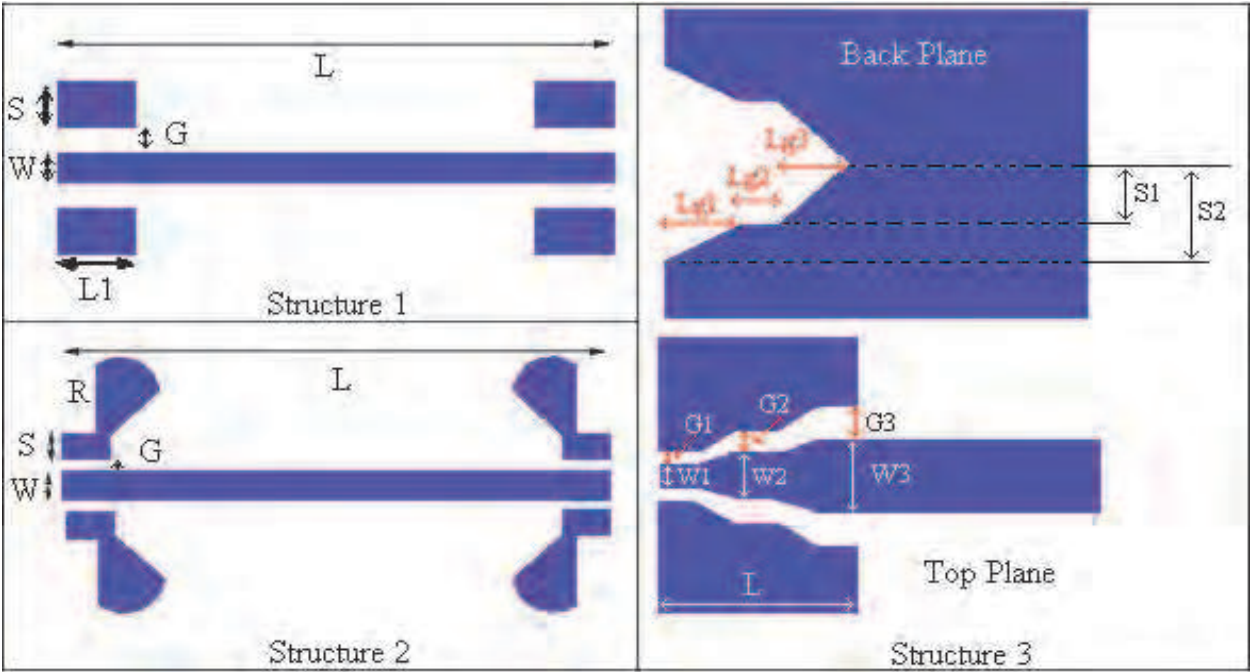Table 1. Dimensions of the studied transition structures in figure 8

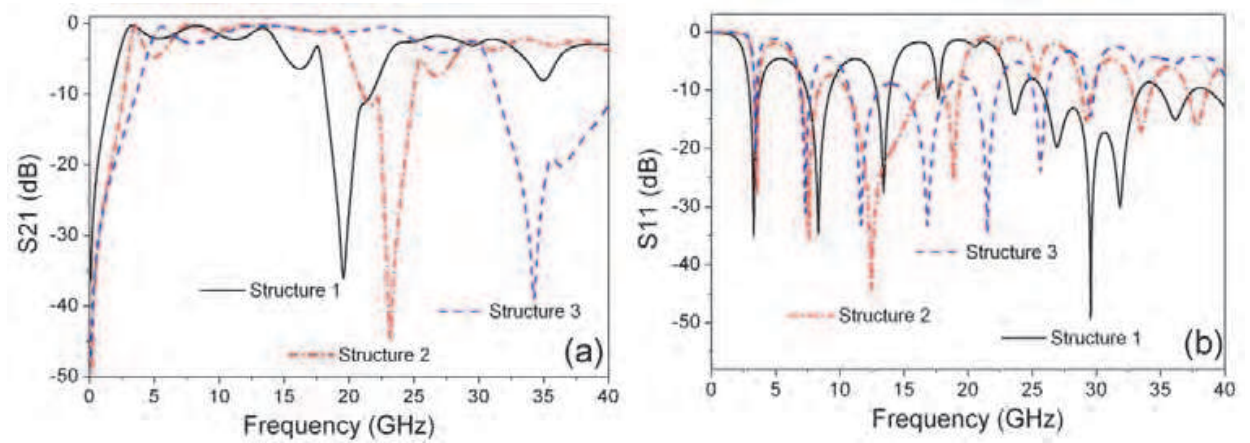Fig. 8. Back-to-back coplanar to microstrip transition structures studied

Fig. 9. HFSS simulations results of different GCPW-MS-GCPW transitions studied; (a) Transmission coefficient S21; (b) Reflection coefficient S11

Figure 9 shows the simulations results of these GCPW-MS-GCPW transitions. As expected, the widest bandwidth is obtained with the structure 3 proposed by Zhu (Zhu & Melde, 2006). However, this transition requires etching the back ground plane, so an additional fabrication step is necessary with careful alignment of the patterns on both sides of the substrate, which complicates the manufacturing process. For the other structures without patterned ground plane, we note that the radial stubs allow to broaden the bandwidth of the structure 2 compared to the structure 1. Nevertheless, the best lower frequency limit of the bandwidth is obtained with the structure 1 because of the large surface of the coplanar pads. Consequently, we chose the structure 1 for our study of vialess GCPW-MS transitions on thin polymer substrates.

Moreover, in the structure 1 the propagating mode in the grounded coplanar line is a quasi-TEM mode. As presented in figure 10, the field chart varies to satisfy the continuity
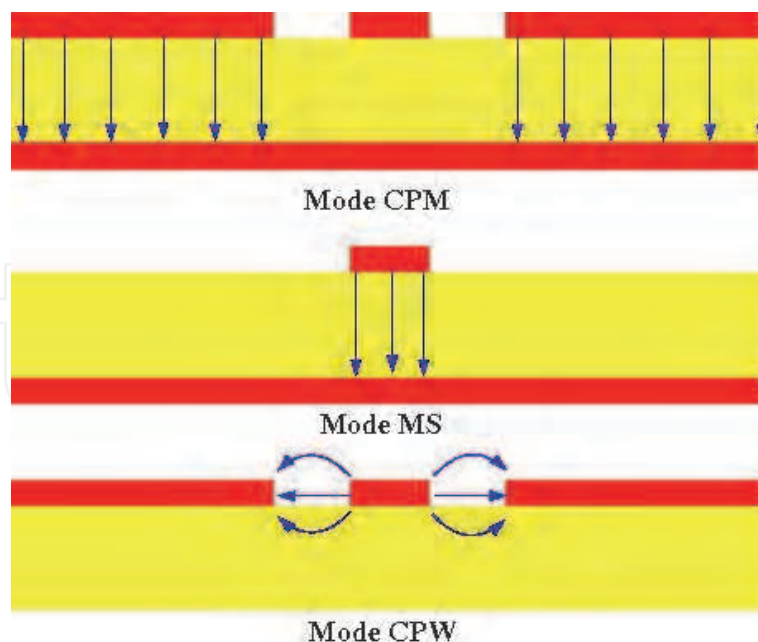
Fig. 10. Electrical field distribution in the GCPW-MS-GCPW transition structure 1

relations. As Raskin proposed in (Raskin et al., 2006), such a structure can propagate three mode configurations: the classical microstrip mode (MS) and coplanar mode (CPW), but also the coplanar microstrip mode (CPM) which diverts incident signal from propagating along the transmission line, resulting in parasitic resonance which limits the transition bandwidth. The transition should be optimized so the applied electrical signal converts rapidly from coplanar mode into microstrip mode on one hand and the excitation of the CPM mode is pushed far in frequency. We will therefore study the influence of the substrate thickness, its relative permittivity and also the surface of the coplanar ground plane the excitation of the CPM mode, both theoretically and experimentally.

3.1.1 Influence of the substrate thickness
To show the influence of the substrate thickness on the bandwidth, we have studied the GCPW-MS-GCPW transition of the structure 1 with three standard thickness of commercial substrate (635 µm, 254 µm and 127 µm). For the electrode, we took a standard copper thickness of 18 µm. And for each thickness, the coplanar width (W) and the coplanar gap (G) of the simulated transition were adjusted to ensure always a characteristic impedance of 50 Ω. And finally, the total length (L) of the back-to-back coplanar microstrip transition was fixed to 2 cm. This value is typically the optimal interaction length between the lightwave and electrical signal in order to minimize the driving voltage of an electro-optical modulator. However, for polymer with high loss tangent and high electro-optical coefficient, this length can be reduced to 1 cm (Gorman, et al., 2009 & Min-Cheol, et al., 2001) while maintaining a low driving voltage. The simulated S-parameters of these three structures are shown in figure 11.

The CPM mode excitation is the origin of the resonance peak at 20 GHz with the 635-µm thick substrate. This resonance peak is rejected to 37 GHz with the 254-µm thick substrate and up to 40 GHz with the 127-µm thick substrate. According to this result, the bandwidth can be increased by decreasing the substrate thickness. So, coplanar to microstrip transitions on thin polymer substrate are expected to have an ultra-wide bandwidth.
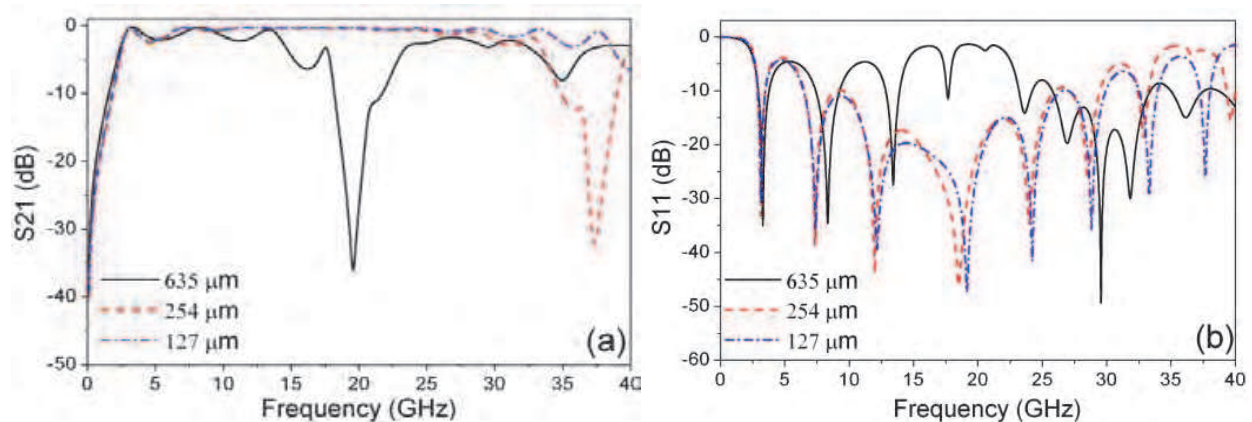
Fig. 11. HFSS simulation results of the GCPW-MS-GCPW transition for different thicknesses; (a) Transmission coefficient S21; (b) Reflection coefficient S11

3.1.2 Influence of geometric parameters

To demonstrate the influence of the geometric parameters of the coplanar to microstrip transition on its bandwidth, figure 12 shows the measured and simulated results of back-to-back coplanar microstrip transitions with two coplanar lengths (L1 = 1 mm and L1 = 5 mm). These transitions are realized on the 254-µm thick NH9338 substrate (ε_r = 3.41 and Tanδ = 0.0047). The other parameters of the transition are fixed to have an impedance matching close to 50 Ω while remaining compatible with the dimensions of the GSG probes we use: the SuSSMicrotec 50A3N500GSG probes (40-GHz bandwidth, 500-µm pitch and 30-µm wide contact pad). Taking into account these constraints, we fixed the following dimensions to realize the transitions: coplanar width W = 530 µm and coplanar gap G = 200 µm.

As shown in figure 12, we obtain, experimentally, a very wide bandwidth with these simple GCPW-MS-GCPW transitions. Indeed, with the coplanar length L1 of 1 mm (figure 12 (a)), the measured (-3 dB) bandwidth extends from 5.5 GHz to 33 GHz. And in the second case, the coplanar length is 5 mm (figure 12 (c)), the transition bandwidth is limited to 12.7 GHz because of the excitation of the CPM mode related to this bigger coplanar length (L1). However, in turn, the lower cutoff frequency is 1.7 GHz whereas this frequency is 5.5 GHz for L1 = 1 mm, because the longer are the coplanar pads, the higher is the capacity between the coplanar ground plane and the bottom ground plane, the better is the electromagnetic coupling between them. However the increase of the coplanar pad surface has drawbacks at high frequencies. Indeed, resonant modes appear at frequencies inversely proportional to their maximum size. So, this parameter is to be optimized according to the desired application. Regarding the reflection coefficient S11, we have experimentally obtained a reflection below -10 dB from 7 GHz and from 1.9 GHz respectively in the case where L1 = 1 mm and L1 = 5 mm (figure 12 (b) and figure 11 (d)). Indeed, a good matching is necessary to ensure optimal power transfer.

We also note a perfect agreement between experimental and simulation results. To obtain this good agreement, the excitation must be modeled exactly as the probes are used to characterize the back-to-back GCPW-MS-GCPW transitions. In HFSS software, we used the lumped port with the exact parameters of our coplanar probes. The skin effect must also be taken into account.
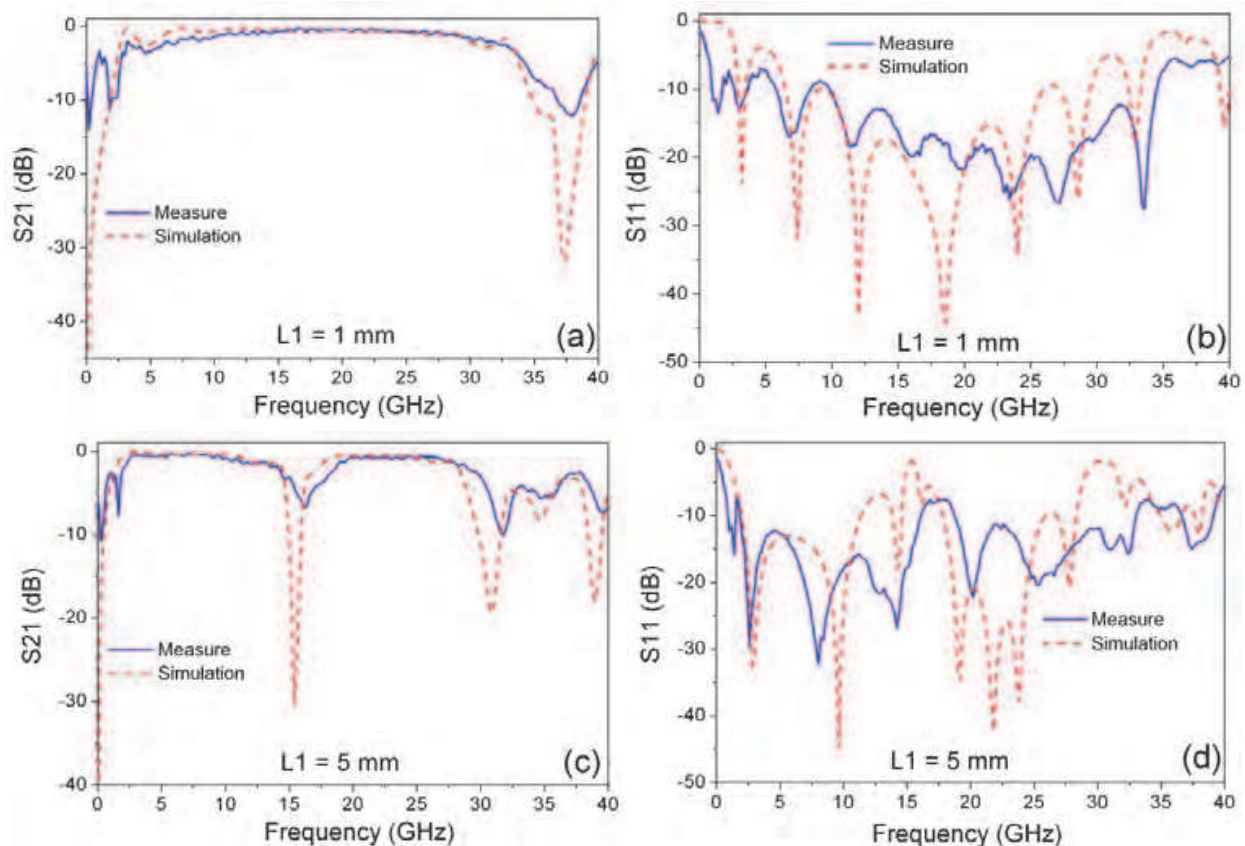
Fig. 12. Measurement and simulation results of the GCPW-MS-GCPW transitions on NH9338 commercial substrate for two coplanar lengths L1; (a) S21 for L1 = 1 mm; (b) S11 for L1 = 1 mm; (c) S21 for L1 = 5 mm; S11 for L1 = 5 mm

3.1.3 Influence of the substrate permittivity

To verify the influence of the substrate permittivity on the bandwidth, the transitions studied are realized with h=254-μm thick standard commercial substrates which have three different permittivities for comparison, RO3003 (ε_r=3, tanδ=0.0013 @ 10 GHz), RO3006 (ε_r=6.15, tanδ=0.0025) and RO3010 (ε_r=10.2, tanδ=0.0035). They are metallized on both sides with 17-μm copper. The dimensions of the transitions are determined in order to maintain a characteristic impedance of 50 Ω for both the microstrip and the grounded coplanar sections. For example, with the substrate RO3003, the width W of the center strip is 615 μm and the coplanar gap G is 185 μm. The length L of the microstrip line is 2 cm. The CPW pads are S=1 mm wide and L1=1 mm long. The measurements and simulations results of these transitions according to the different permittivities (Figure 13) show that when the relative permittivity is low, the resonance peak appears at higher frequencies. Thus, the high cut-off frequency of the transitions due to the first parasitic resonance is respectively 20.6, 25 and 33.4 GHz for substrates of permittivities of 10.2, 6.15 and 3. Due to the electromagnetic coupling between the backside conductor and the coplanar ground strips, the low cut-off frequency increases with decreasing permittivity, respectively to 1.7, 2.4 and 4 GHz. Indeed, low permittivity obtained by micromachining substrates allows to get low-dispersive waveguides (quasi TEM approximation) and to realize coplanar transmission lines with very high bandwidth without excessive dispersion and loss (Newham, 2006). The main

reason for the high cut-off frequency improvement of GCPW-MS-GCPW transitions is that the guided wavelength is bigger in low-k substrate for a given frequency, so the parasitic resonance between the backside conductor and the coplanar ground strips takes place at higher frequency (El-Gibari, et al., 2010a). In addition, as for low effective permittivities a large part of the energy is propagating in air medium, so losses can be minimized.
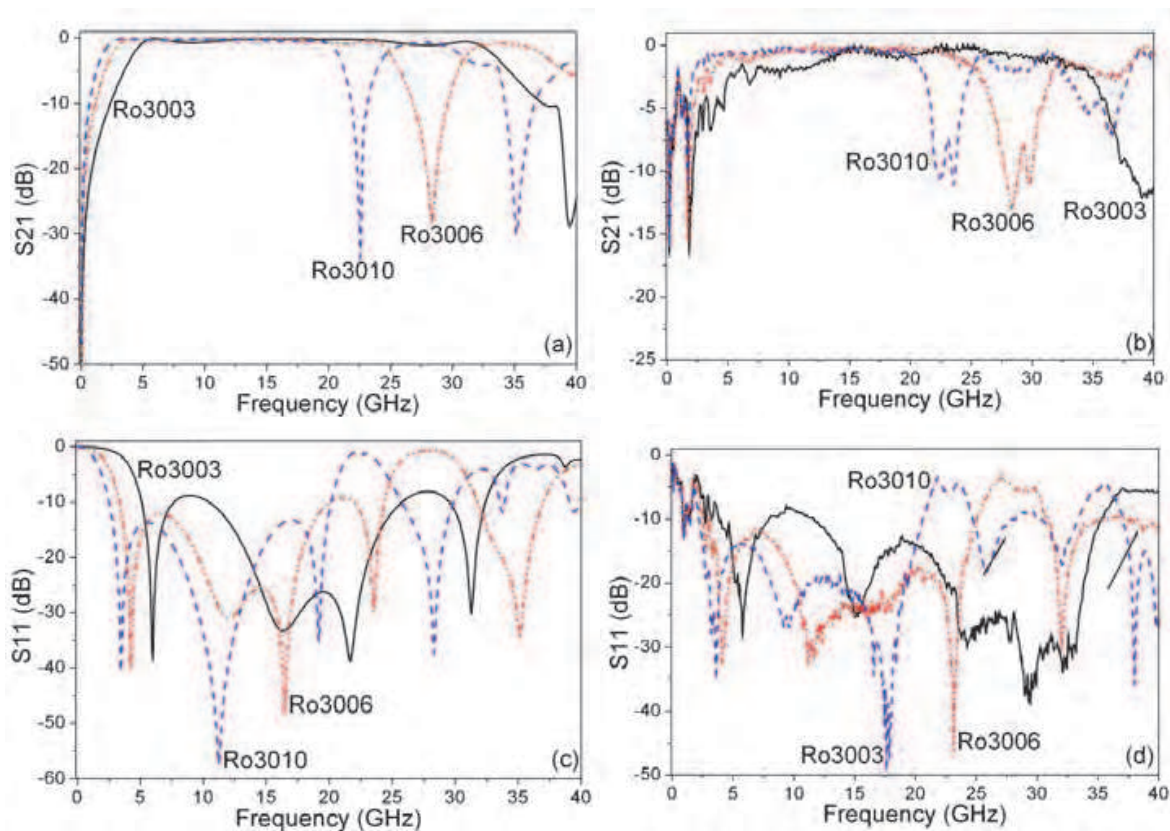

Fig. 13. Calculated and measured S-parameters of back-to-back GCPW-MS-GCPW transition on 254-μm substrates with different permittivities; (a) S21 simulated; (b) S21 Measured; (c) S11 simulated; (d) S11 Measured;

3.2 GCPW-MS-GCPW transitions on thin polymer substrate

For our study of GCPW-MS-GCPW transitions on thin film substrate, we have chosen the commercial benzocyclobutene polymer (BCB), often used in microelectronic packaging and interconnection applications, it is an excellent candidate as substrate in thin film for GCPW-MS-GCPW transitions, with its remarkable features: low-permittivity (ε_r=2.65), low loss tangent (tanδ=0.0025), simple and cost-effective to deposit, varying thickness through the spinning-curing process, resistant to some chemical agents, etc.. In order to reduce the driven voltage of the modulator, the thickness of thin film polymer is fixed usually between 8 μm (El-Gibari, et al., 2010b) and 10 μm (Michalak, et al., 2006). So, our transitions are realized on 10-μm BCB polymer. The first study in thin film consists to determine the influence of the coplanar length (L1). Our study consists to fix the coplanar width S at 1 mm and varying its length L1 (1, 2 and 3 mm). For the metal electrode, we used aluminum which can be deposited in our laboratory. The width of the central strip W = 20 μm, the coplanar gap G = 13 μm and the length (L) of the back-to-back transition is fixed at 1 cm.

3.2.1 Influence of the coplanar length L1

Figure 14 (a) presents the evolution of the transmission coefficient S21 of the back-to-back transition according to the coplanar length (L1) for a fixed coplanar width (S) at 1 mm. This study was realized without taking into account the loss tangent of the BCB polymer. As in the case of the thick substrate, the appearance of the resonance frequency due to the excitation of the CPM mode depends on the coplanar length (L1). When this length is short, this resonance peak is rejected at high frequencies. For example, when L1 = 1 mm, the first resonance peak appears around the frequency of 78 GHz, whereas it appears around 29 GHz with L1 = 3 mm. Moreover, the lower cut-off frequency of the bandwidth depends on the total surface of the coplanar pads (S.L1). The larger is this surface, the greater is the capacitive effect between the ground plane of the microstrip line and the top ground plane of the coplanar line, the more the lower limit of the bandwidth decreases. Thus, this lower cut-off frequency is at 230 MHz with L1 = 3 mm and at 670 MHz with L1 = 1 mm. Regarding the reflection, figure 14 (b) shows a good matching with a reflection coefficient S11 less than - 10 dB from 460 MHz.
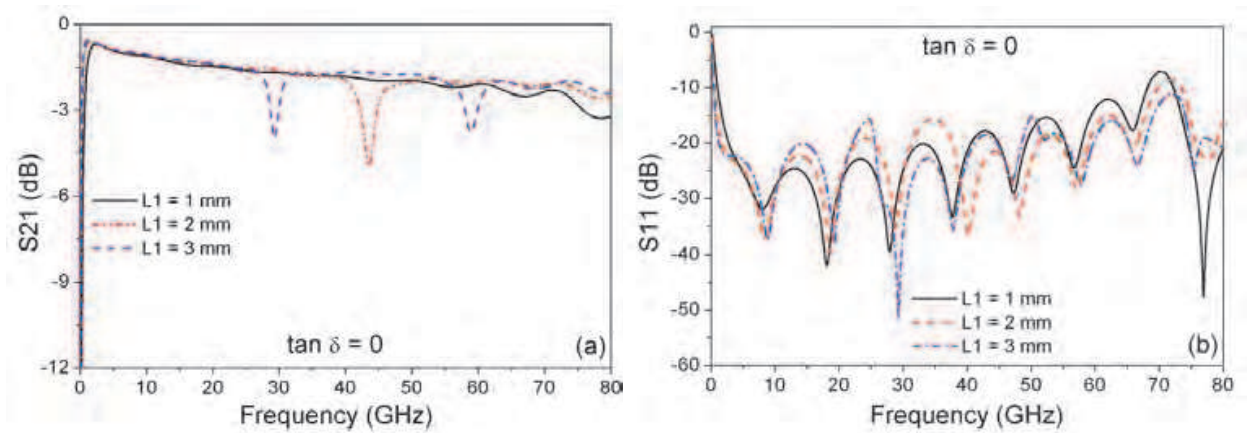

Fig. 14. S-parameters of the back-to-back transition according to the coplanar length (L1); (a) Transmission coefficient S21; (b) Reflection coefficient S11

Table 2 contains the GCPW-MS-GCPW transition bandwidth higher and lower limits. One can extend the transition bandwidth to higher frequency be decreasing the length of the coplanar pads or on the contrary push its lower limit towards DC component by increasing the length of the coplanar pads.

L1 (mm)	Tanδ	Lower cut-off frequency (MHz)	High frequency (GHz)	-3 dB bandwidth (GHz)
1		670	75,8	≈ 75
2	0	340	42,2	≈ 43
3		230	28,6	≈ 28,5

Table 2. The transition bandwidth depending on the length of the coplanar pads L1 with the width S fixed at 1 mm.

To understand the physical phenomenon underlying microwave properties of the studied transitions, we present in figure 15 the evolution of the electric field propagating along the transition at 1 GHz. The small thickness of the BCB polymer presents a double advantage for a good via-less transition. On one hand, it can easily create an electromagnetic coupling between the bottom ground plane of the microstrip line and the coplanar pads by capacitive effect. On the other hand, the low ratio of the thickness and the coplanar gap allows a fast conversion of the field between the coplanar mode and microstrip mode. This is well illustrated by figure 15 (a) showing the electric field at the input of the first transition in plane 1. The energy propagates in coplanar and microstrip modes. These two modes are coupled (figure 16) and the coupling is all the stronger as the capacity between the coplanar pad and the bottom ground plane is large. Thus, the energy is quickly confined under the central strip. In our case, the coplanar gap (G = 13 µm) is greater than the thickness of the BCB polymer (h = 10 µm). The mode "sees" first the ground plane of the microstrip line which facilitates the fast conversion between the coplanar mode and the microstrip mode. This remark seems to be justified by observing the electric field at the output of the first transition in Figure 15 (b). We note that the mode installed is of microstrip type: the maximum of energy is confined under the central strip. Thus on figure 15 (c), we have a quasi-TEM mode which corresponds to the mode propagating along the microstrip line. In figure 15 (d) which presents the electric field in the input of the second transition, we find the phenomenon of the first plane, where the propagating mode is a hybrid mode between the coplanar and the microstrip modes with a maximum of energy confined under the central strip thanks to the low thickness of the substrate.
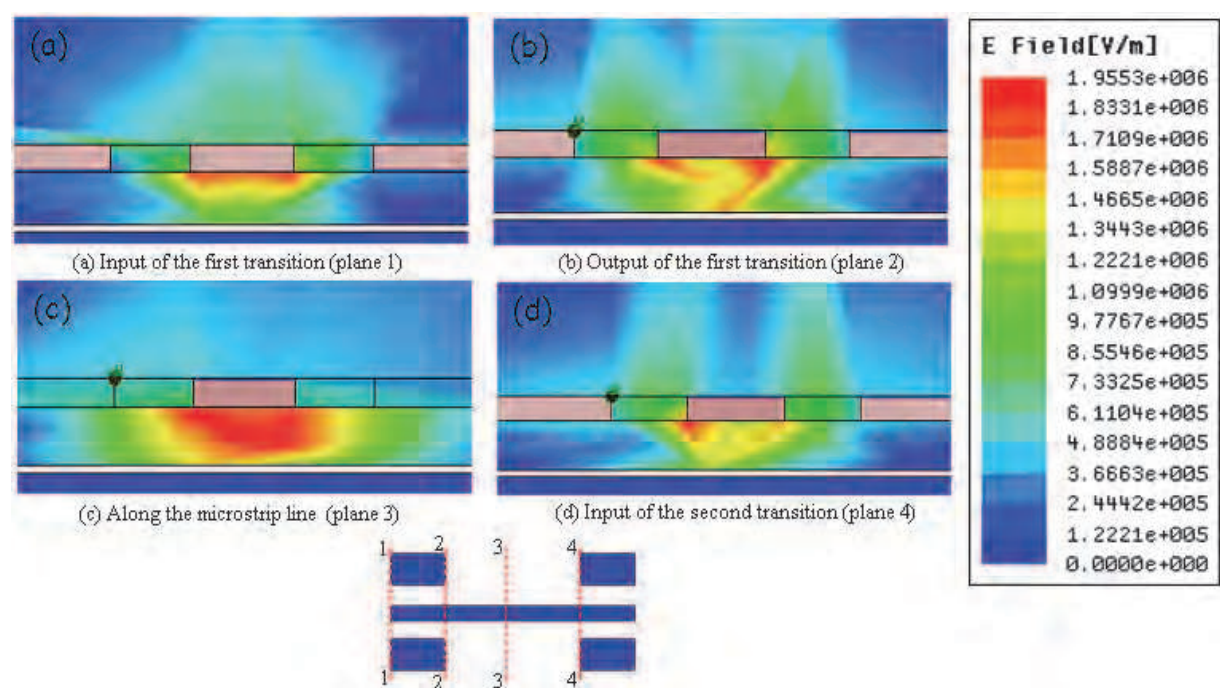

Fig. 15. Representation of the electric field at 1 GHz in several transverse planes of the GCPW-MS-GCPW transition

The physical phenomenon which we explained in the previous paragraph remains valid whatever the frequency of the wave propagating in the structure, except for those frequencies at which the CPM mode is excited. In the structure studied, the excitation of this
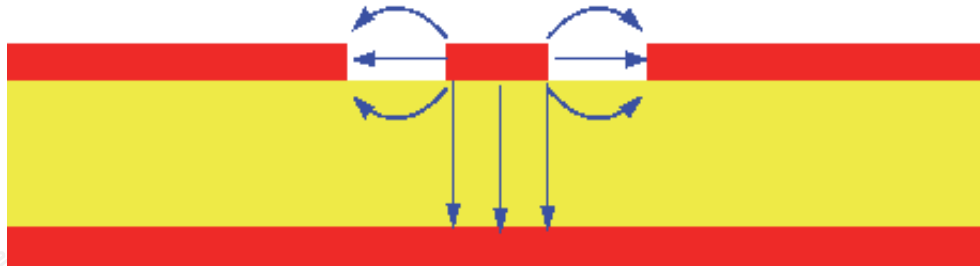
Fig. 16. Distribution of the field at the input of the GCPW-MS-GCPW transition (plane 1)

CPM mode takes place around a frequency of 43 GHz (figure 14). Figure 17 shows the cartography of the electric field at the frequency corresponding to this resonance peak. The energy is clearly directed towards between the coplanar ground plane and the microstrip ground plane instead of propagating along the center strip, resulting in a drop of the S21 parameter hence bandwidth limitation.
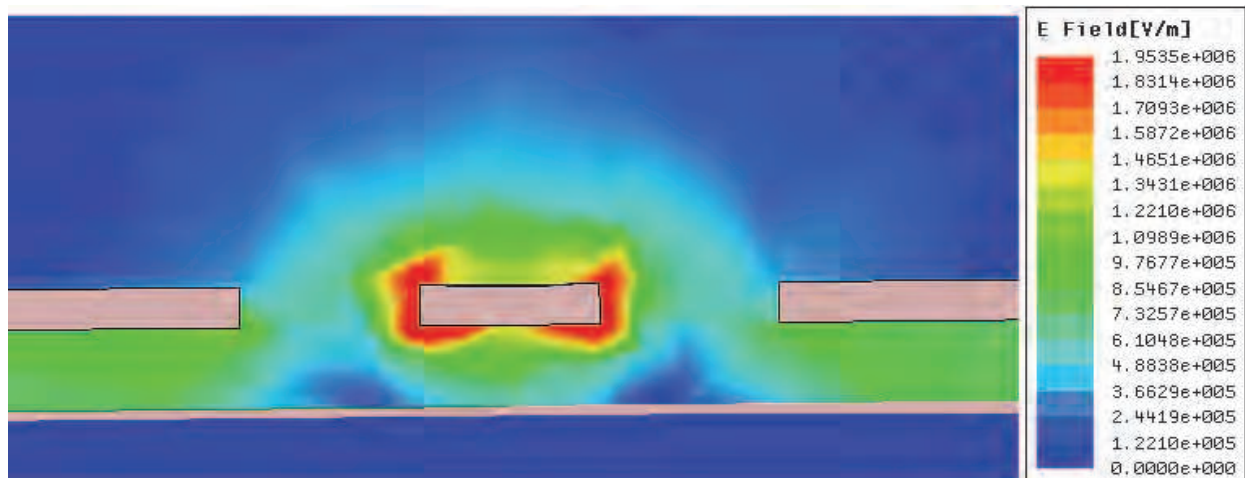

Fig. 17. Representation of the electric field at 43 GHz in the input of the GCPW-MS-GCPW transition (plane 1)

3.2.2 Realization of the GCPW-MS-GCPW transitions on BCB polymer

For experimental characterization of our structures on polymer thin film, we used a network analyzer Agilent E8364B whose bandwidth covers the frequency range from 10 MHz to 50 GHz, using the LRM (Line-Reflect-Match) calibration technique. The system is controlled by the Wincal Cascade software. For the GSG coplanar probes, we used the Cascade I40AGSG250 probes (40 GHz bandwidth, 250 µm pitch and 12 µm pad). Finally, the probes are calibrated using a calibration substrate referenced by Cascade AE-101-190.

We present in figure 18 the measurement and simulation results obtained with 10-µm BCB polymer substrate, deposited by spin-coating on a 380 µm thick metallized silicon wafer. We have realized two transitions with different aluminum thicknesses in order to show its influence. So, Figure 18 (a) presents the measurement and simulation results of the GCPW-MS-GCPW transition realized with 0.4 µm of aluminum thickness. We can notice that the insertion loss of the transition is as high as 3 dB due to the ohmic effect of the thin metal layer. In figure 18 (b) the aluminum thickness deposited and measured with a profilometer

is 1.4 µm, in this case we experimentally obtained a very large (-3 dB) bandwidth from 700 MHz to 22.5 GHz. We also note that S21-parameter curve has a very low slope thanks to the very low loss tangent of the BCB polymer and the use of a metallized silicon wafer. A good impedance matching can be also observed in figure 18 (b). Similarly, a very good agreement between the experimental and simulation results is obtained.
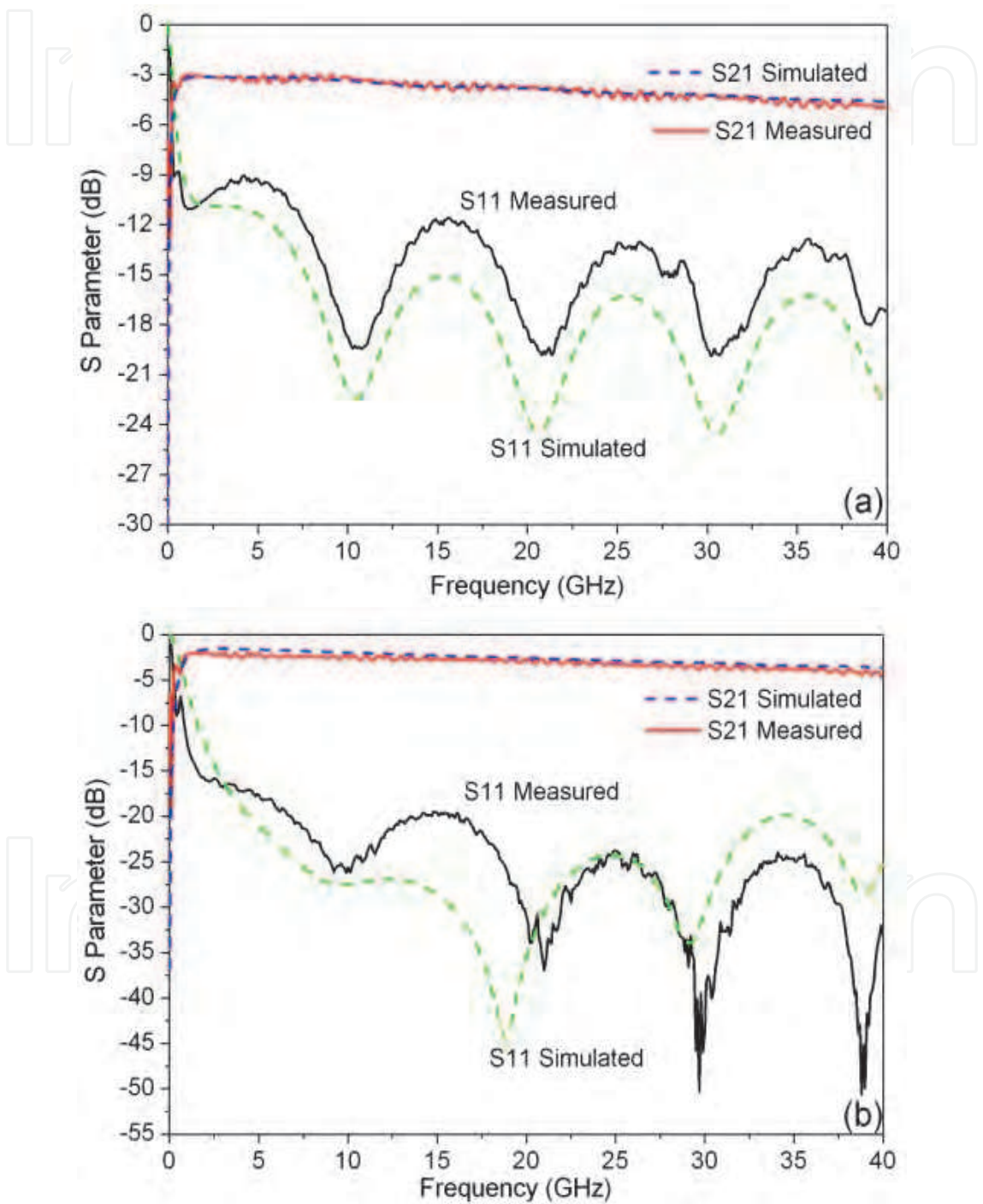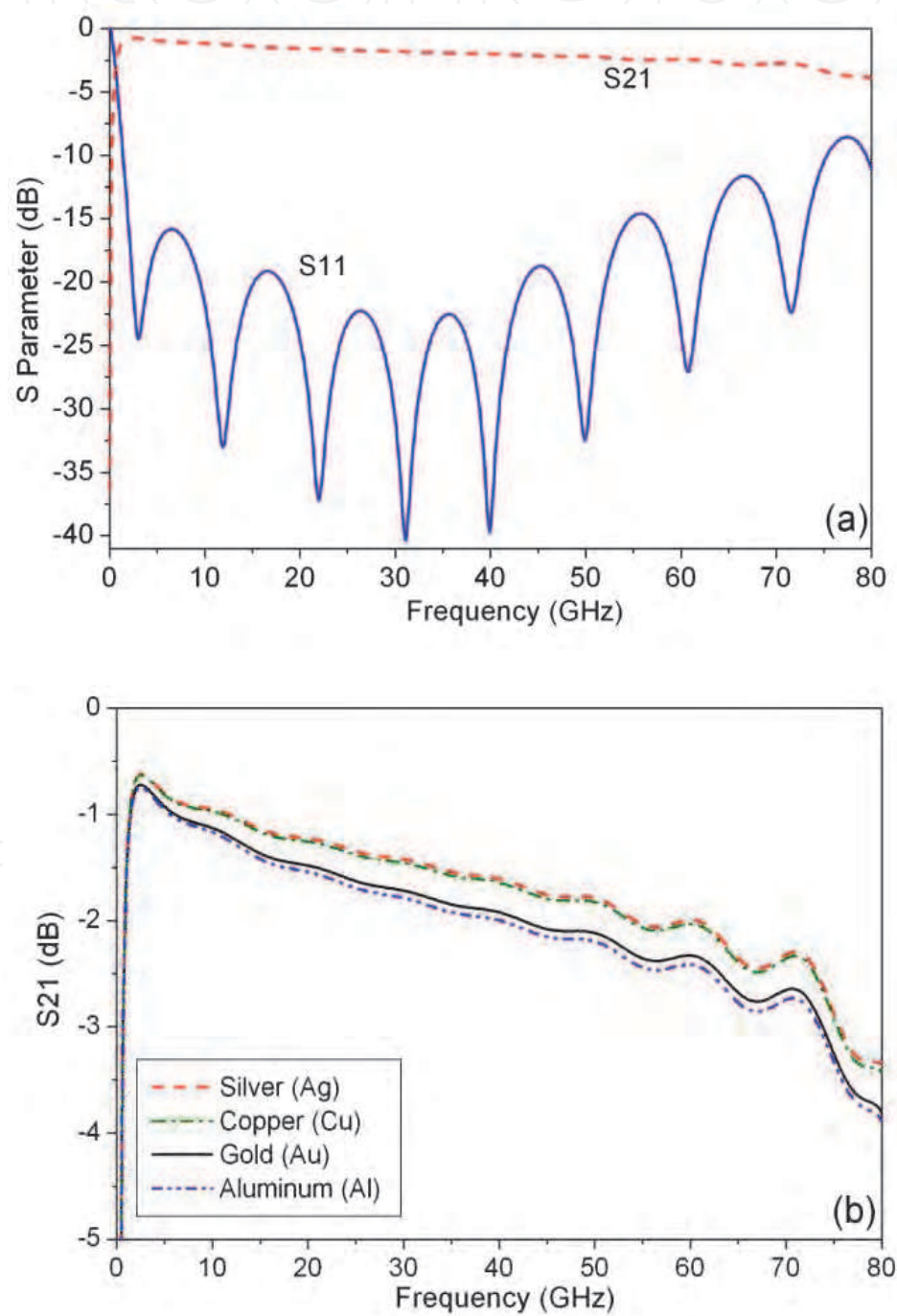

Fig. 18. Measured and simulated S-parameters of a back-to-back GCPW-MS-GCPW transition on BCB polymer substrate; (a) with 0.4 µm aluminum metallization, (b) with 1.4 µm aluminum metallization.

The low metallization thickness is one the main contributor for the losses observed in the GCPW-MS-GCPW transitions presented previously. The simulations results on BCB polymer, presented in figure 19 (a), show that an ultra-wide bandwidth (72 GHz) could be obtained by increasing the metal thickness up to 4 μm. The other conditions of simulations in this study are: W = 20 μm, G = 13μm, S = 1 mm and L1 = 1mm.

Another manner to increase the bandwidth of the GCPW-MS-GCPW transitions is to choose a metal with a higher conductivity. Figure 19 (b) shows the simulation results of the transition on BCB polymer with different metals. The bandwidth can be increased by 4 GHz if aluminum is replaced by silver.
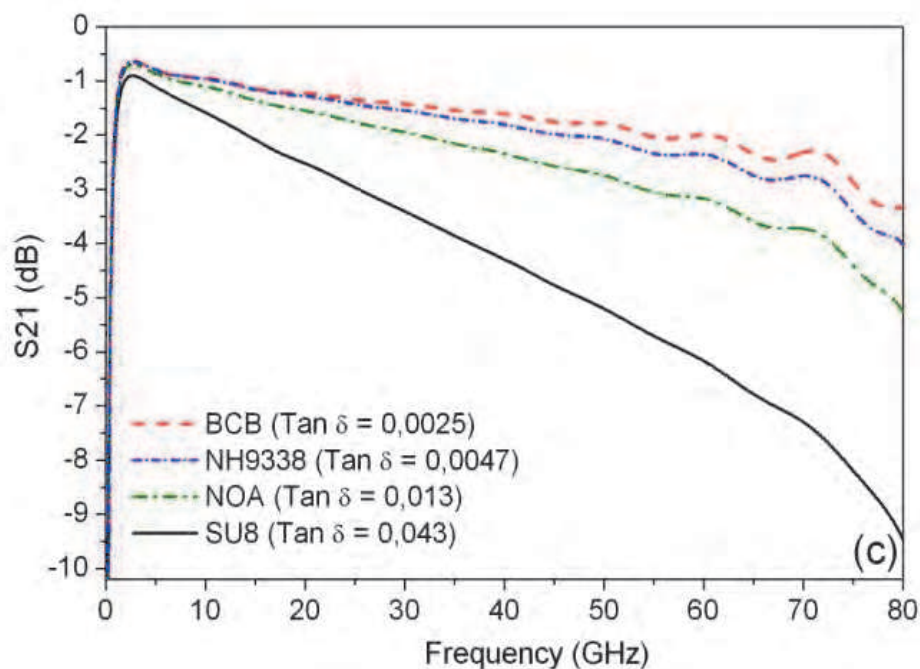
Fig. 19. S-parameters of a back-to-back GCPW-MS-GCPW transition on 10-μm thick BCB polymer substrate; (a) with 4 μm thick aluminum metallization, (b) different electrode metals (c) different substrate materials.

Another way to increase the transitions bandwidth is to use materials with low loss tangent. For example, figure 19 (c) presents the simulation results of the transition with different loss tangent of materials. For all transitions whose S-parameters are shown in figure 19, 4 μm thick metallization was assumed. The dielectric loss and metal conductivity modifies differently the transition bandwidth, the first impacts the S21 parameter slope and the second influences the insertion losses.

3.3 Transitions for connectorizing the component

For the packaging of component driven by microstrip line on thin substrate, a GCPW-MS-GCPW transition is necessary for connectorizing with a coplanar connector. For this, we chose the end launch coplanar connector, Model #1492-04A-5 of SouthWest Microwave. The diameter of its center contact is 127 μm and its coplanar gap is 254 μm. So, the center conductor width and the coplanar gap of the transition must be sufficiently large to easily install the connector.

To reduce the driving voltage of the modulator, the thickness of BCB polymer having been fixed at 10 μm, a segmentation of the bottom ground plane is needed to maintain the impedance matching when the width of the center conductor increases. Most of the transitions used in the literature are based on a smooth transformation of the field by gradually changing the physical boundary conditions (Zhu & Melde, 2006), so the characteristic impedance is maintained at 50 Ω in all sections of the transition.

The proposed transition for connectorization with the coplanar connector is shown in figure 20. In this transition, W_1, W_2 and W_3 indicate the different widths of the signal conductor in different sections, G_1, G_2 and G_3 indicate the different values of the coplanar gap, L1 the length of the coplanar line and the L2 the length of the grounded coplanar line. For each

section, the width of the signal conductor on the top plane gradually decreases from the width needed for the coplanar connector to the final width of the microstrip line optimized to have a characteristic impedance of 50 Ω. At the beginning of the transition, the bottom ground is designed to have a tapered slot. This is necessary to facilitate the excitation of the coplanar fundamental mode and a gradual installation of the microstrip fundamental mode at the grounded coplanar line. This is possible thanks to the thinness of the BCB polymer lower than the coplanar gap.
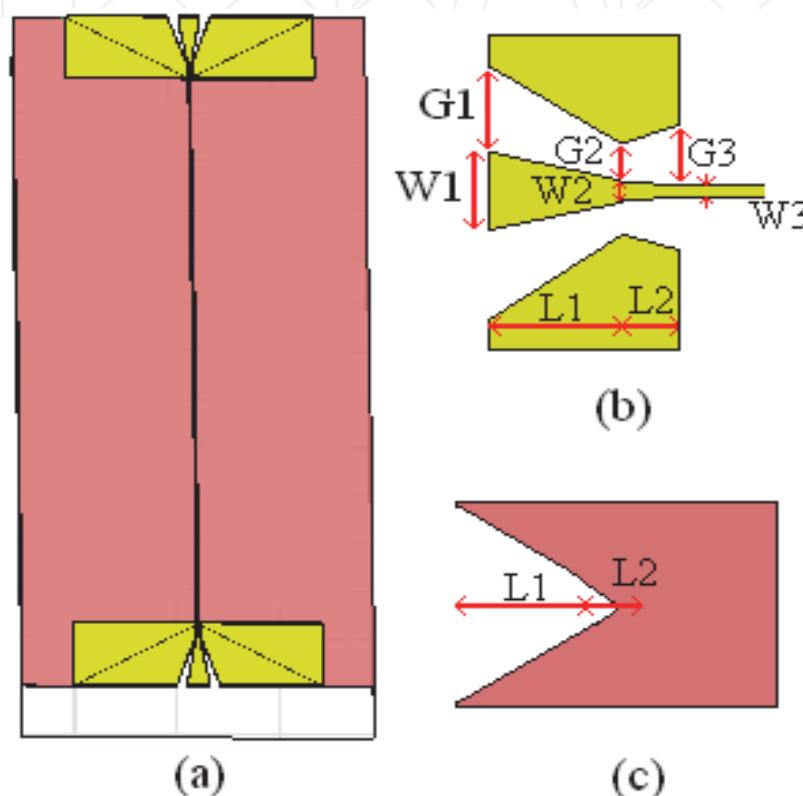
Fig. 20. Structure of the GCPW-MS-GCPW transition for connectorizing with coplanar connectors. (a) Global view of the transition studied. (b) View of the top metallization pattern of the taper. (c) View of the bottom ground plane

For mechanical fixing on the substrate, the end launch connector is equipped with screws in its corners. So, for our application we take advantage of these holes in order to obtain the DC contact. We used the RT/Duroid 6010 substrate which has a permittivity similar to that of silicon wafer, with which we studiez transitions. So, the transition was designed on BCB polymer (10 µm of thickness, ε_r=2.65 and tanδ= 0.0025) deposed on RT/Duroid 6010 substrate (635 µm of thickness, ε_r=10.2 and tanδ= 0.0035). The signal line widths were determined first. The value of W_3 was determined to have a microstrip characteristic impedance of 50 Ω. This width depends essentially on the thickness of BCB polymer deposed (10 µm) and its permittivity (2.65). So, W_3 is fixed at 20 µm. Secondly, to simplify the installation of the coplanar connector, we fixed the value of W_1 at 220 µm. We design a smooth transition by gradually changing the physical boundary conditions, so insertion losses are minimized. Simulations were realized for several different cases, the parameters of the most efficient transition are as follows: W_1 = 220 µm, G_1 = 110 µm, W_2 = 30 µm, G_2 = 8 µm. The coplanar gap becomes critical to maintain the characteristic impedance at 50 Ω.

Starting from W_2 we consider the area of grounded coplanar line, $W_3 = 20$ µm, $G_3 = 13$ µm. In order to achieve a progressive transition, the coplanar lengths L1 and L2 are chosen to minimize the losses due to the fast change of the widths of the coplanar line (from 220 µm to 20 µm). According to the various simulations realized, we took 1 mm and 300 µm respectively for L1 and L2. The total length (L) of the back-to-back transition is 15 mm in order to facilitate the placement of the coplanar connector. Figure 21 shows that a very broad bandwidth from 700 MHz to 32 GHz is achieved with the station system equipped with GSG probes, and for the coplanar connector we are working to realize this transition.
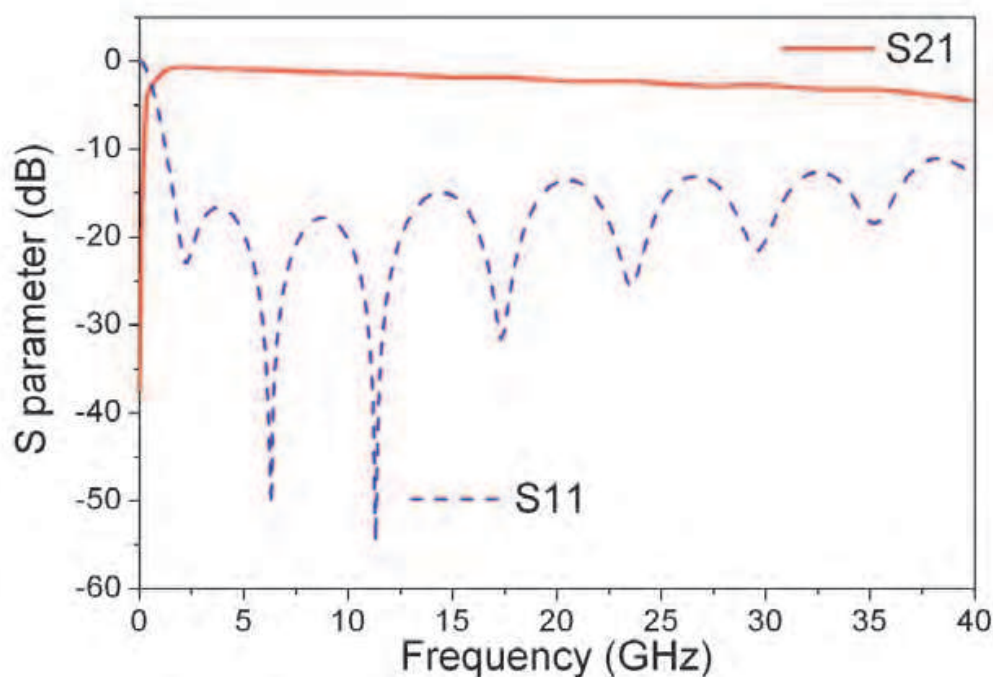

Fig. 21. Calculated S-parameters of back-to-back GCPW-MS-GCPW transition on BCB polymer deposed on RT/Duroid 6010 substrate

4. Conclusion

We present an ultra-wide bandwidth back-to-back GCPW-MS-GCPW transition without making via-hole in the substrate or patterning the bottom ground plane. These transitions, using the electromagnetic coupling between the bottom and top ground planes, simplifies the manufacturing and facilitates the on-wafer characterization with GSG probe station. These transitions are widely requested in packages, on-wafer measurements of microstrip based MMICs, and also in the interconnections in hybrid circuit including both microstrip and coplanar lines.

Low permittivity and thin substrates permit rejecting of the CPM mode resulting from parasitic resonance between backside conductor and planar ground strips, so enlarging the bandwidth of back-to-back GCPW-MS-GCPW transitions. As is shown by the measurements and simulations results, we have obtained a very wide bandwidth exceeding 30 GHz with the NH9338 substrate ($\varepsilon_r = 3.41$, Tan$\delta = 0.0047$ and thick = 254 µm) and with the BCB polymer ($\varepsilon_r = 2.65$, Tan$\delta = 0.0025$ and thick = 10 µm), and a bandwidth from 700 MHz to 22.5 GHz.

Simulation results with the BCB polymer show that the bandwidth could go beyond 76 GHz, which opens the perspectives of cost-effective electro-optical modulator based on polymer. This last has an enormous potential bandwidth thanks to a good optical-microwave phase match in polymers over 100 GHz, while that of their counterparts made of $LiNbO_3$ is limited to about 40 GHz. They need absolutely an electrode with a very wide bandwidth.

5. Acknowledgment

6. References

Algani, C.; Belhadj-Tahar, N. E.; Deshours, F.; Montmagnon, J. L.; Roduit, P.; Alquié, G.; Fortin, C. & Kazmierski, C. (2005). Optimization of the electrode dimensions of an electro-optic organic modulator based on polymers microwave dielectric characterization and electromagnetic simulations. *European Microwave Conference*, Vol. 2, 4 pp. (4-6 October 2005), ISBN 2-9600551-2-8

Chen, D.; Fetterman, H. R.; Chen, A.; Steier, W.H.; Dalton, L. R.; Wang, W. & Shi, Y. (1997). Demonstration of 110 GHz electro-optic polymer modulators. Appl. Phys. Lett., Vol.70, No.25, (June 1997), pp. 3335-3337

Courjal, N.; Porte, H.; Martinez, A. & Goedgebuer, J.P. (2002). $LiNbO_3$ Mach-Zehnder modulator with chirp adjusted by ferroelectric domain inversion. *IEEE Photonics Technology Letters*, Vol.14, No.11, (November 2002), pp. 1509, ISSN 1041-1135

Dalton, L. R.; Harper, A.; Ren, A.; Wang. F. F.; Todorova, G.; Chen, J.; Zhang, C. & Lee, M. (1999). Polymeric electro-optic modulators : From chromophore design to integration with semiconductor very large scale integration electronics and silica fiber optics. *Industrial & Engineering Chemistry Research*, Vol.38, No.1, (January 1999), pp. 8-33

El-Gibari, M.; Averty, D.; Lupi, C.; Brunet, M.; Li H. W.; & Toutain, S. (2010a). Ultra-broad bandwidth and low-loss GCPW-MS transitions on low-k substrates. *Electronics Letters*, Vol.46, No.13, (June 2010), pp. 931, ISSN 0013-5194

El-Gibari, M.; Averty, D.; Lupi, C.; Li H. W. & Toutain, S. (2010b). Ultra-wideband GCPW-MS-GCPW driven electrode for low-cost and wide range application electro-optic modulators. *Microwave and Optical Technology Letters*, Vol.52, No.5, (May 2010), pp. 1078-1082

Faderl, L. ; Labeye, P. ; Gidon, P. & Mottier, P. (1995). Integration of an electrooptic polymer in an integrated optics circuit on silicon. IEEE *Journal of Lightwave Technology*, Vol.13, No.10, (October 1995), pp. 2020, ISSN 0733-8724

Gauthier, G. P.; Katehi, L. P. & Rebeiz, G. M. (1998). W-Band finite ground coplanar waveguide (FGGPW) to microstrip line transition. *IEEE MTT-S International Microwave Symposium Digest*, Vol. 1, pp. 107-109 (7-12 June 1998), ISBN: 0-7803-4471-5

Gorman, T.; Haxha, S. & Ju, J. J. (2009). Ultra-High-Speed Deeply Etched Electrooptic Polymer Modulator With Profiled Cross Section. *IEEE Journal of Lightwave Technology*, Vol.27, No.1, (January 2009), pp. 68, ISSN 0733-8724

Hammerstad, E. O. (1975). Equations for Microstrip Circuit Design. *European Microwave Conference,* pp. 268-272, (1-4 September 1975)

Haydl, W.H. (2002). On the use of vias in conductor-backed coplanar circuits. *IEEE Transactions on Microwave Theory and Techniques,* Vol.50, No.6, (June 2002), pp. 1571, ISSN 0018-9480

Kim, I.; Tan, M.R.T. & Wang, S.-Y. (1990). Analysis of a new microwave low-loss and velocity-matched III-V transmission line for traveling-wave electrooptic modulators. *IEEE Journal of Lightwave Technology,* Vol.8, No.5, (May 1990), pp. 728, ISSN 0733-8724

Lee, Y. C. & Park, C. S. (2006). Vialess Coplanar Probe Pad-to-Microstrip Transitions for 60 GHz-band LTCC Applications. *European Microwave Conference,* pp. 1354, (10-15 September 2006), ISBN 2-9600551-6-0

Michalak, R.J. ; Ying-Hao Kuo ; Nash, F.D. ; Szep, A. ; Caffey, J.R. ; Payson, P.M. ; Haas, F. ; McKeon, B.F. ; Cook, P.R. ; Brost, G.A. ; Jingdong Luo ; Jen, A.K.-Y. ; Dalton, L.R. ; Steier, W.H. (2006). High-speed AJL8/APC polymer modulator. *IEEE Photonics Technology Letters,* Vol.18, No.11, (June 2006), pp. 1207, ISSN 1041-1135

Min-Cheol, O; Zhang, H.; Zhang, C.; Erlig, H.; Chang, Y.; Tsap, B.; Chang, D.; Szep, A.; Steier, W. H.; Fetterman, H. R. & Dalton, L. R. (2001). Recent advances in electrooptic polymer modulators incorporating highly nonlinear chromophore", *IEEE Journal of Selected Topics in Quantum Electronics,* Vol.7, No.5, (September 2001), pp. 826, ISSN 1077-260X

Newham, P. (2006). Coupling across gap in thick microstrip line. *IEE Proceedings H, Microwaves, Antennas and Propagation,* Vol.136, No.1, (May 2005), pp. 64, ISSN 0950-107X

Raskin, J. P.; Gautier, G.; Katheli, L. P. & Rebeiz, G. M. (2000). Mode conversion at GCPW-to-microstrip-line transitions. *IEEE Transactions on Microwave Theory and Techniques,* Vol.48, No.1, (January 2006), pp. 158, ISSN 0018-9480

Safwat, M. E.; Zaki, K. A.; Johnson, W. & Lee, C. H. (2002). Novel Transition Between Different Configurations of Planar Transmission Lines", *IEEE Microwave and Wireless Components Letters,* Vol.12, No.4, (April 2006), pp. 128-130

Straub, G.; Ehret P. & W. Menzel. (1996). On-wafer measurement of microstrip-based MIMICs without via holes. *IEEE MTT-S International Microwave Symposium Digest,* Vol. 3, pp. 1399 (17-21 June 1996), ISBN: 0-7803-3246-6

Wheeler, H.A. (1977). Transmission-Line Properties of a Strip on a Dielectric Sheet on a Plane. *IEEE Journal of Lightwave Technology,* Vol.25, No.8, (August 1977), pp. 631, ISSN 0018-9480

Zheng, G.; Papapolymerou, J. & Tentzeris, M. M. (2003). Wideband coplanar waveguide RF probe pad to microstrip transitions without via holes. *IEEE Microwave and Wireless Components Letters,* Vol.13, No.12, (December 2006), pp. 544-546, ISSN 1531-1309

Zhu, L. & Melde, K. L. (2006). On-Wafer Measurement of Microstrip-Based Circuits With a Broadband Vialess Transition. *IEEE Transactions on Advanced Packaging,* Vol.29, No.3, (August 2006), pp. 654, ISSN 1521-3323
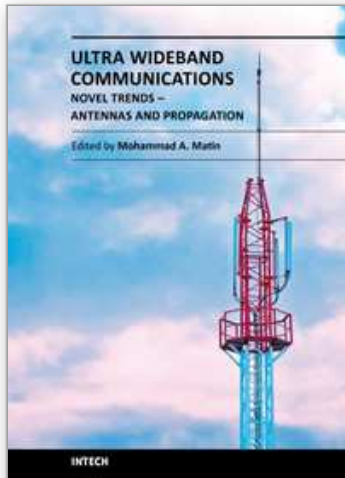
Ultra Wideband Communications: Novel Trends - Antennas and Propagation

Edited by Dr. Mohammad Matin

This book explores both the state-of-the-art and the latest achievements in UWB antennas and propagation. It has taken a theoretical and experimental approach to some extent, which is more useful to the reader. The book highlights the unique design issues which put the reader in good pace to be able to understand more advanced research.

How to reference

In order to correctly reference this scholarly work, feel free to copy and paste the following:

Mohammed El-Gibari, Dominique Averty, Cyril Lupi, Yann Mahé Hongwu Li and Serge Toutain (2011). Coplanar-Microstrip Transitions for Ultra-Wideband Communications, Ultra Wideband Communications: Novel Trends - Antennas and Propagation, Dr. Mohammad Matin (Ed.), ISBN: 978-953-307-452-8, InTech, Available from: http://www.intechopen.com/books/ultra-wideband-communications-novel-trends-antennas-and-propagation/coplanar-microstrip-transitions-for-ultra-wideband-communications

INTECH
open science | open minds